HHS Public Access

Author manuscript

*Mitochondrial Commun*. Author manuscript; available in PMC 2024 September 05.

Published in final edited form as:

*Mitochondrial Commun*. 2023 ; 1: 48–61. doi:10.1016/j.mitoco.2023.08.001.

# Structure-destabilizing mutations unleash an intrinsic perforation activity of antiapoptotic Bcl-2 in the mitochondrial membrane enabling apoptotic cell death

**Ping Gao**[a,1], **Zhi Zhang**[b,1], **Rui Wang**[a,1], **Li Huang**[a,1], **Hao Wu**[a], **Zhenzhen Qiao**[c], **Xiaohui Wang**[a], **Haijing Jin**[a], **Jun Peng**[b], **Lei Liu**[a], **Quan Chen**[a,c,**], **Jialing Lin**[b,d,*]

[a]The State Key Laboratory of Membrane Biology, Institute of Zoology, Chinese Academy of Sciences, Beijing, 100101, China

[b]Department of Biochemistry and Molecular Biology, University of Oklahoma Health Sciences Center, Oklahoma City, OK, 73126, USA

[c]College of Life Sciences, Nankai University, Tianjin, 300071, China

[d]Stephenson Cancer Center, Oklahoma City, OK, 73104, USA

## Abstract

Bcl-2 and Bax share a similar structural fold in solution, yet function oppositely in the mitochondrial outer membrane (MOM) during apoptosis. The proapoptotic Bax forms pores in the MOM to trigger cell death, whereas Bcl-2 inhibits the Bax pore formation to prevent cell death. Intriguingly both proteins can switch to a similar conformation after activation by BH3-only proteins, with multiple regions embedded in the MOM. Here we tested a hypothesis that destabilization of the Bcl-2 structure might convert Bcl-2 to a Bax-like perforator. We discovered that mutations of glutamate 152 which eliminate hydrogen bonds in the protein core and thereby reduce the Bcl-2 structural stability. These Bcl-2 mutants induced apoptosis by



*Corresponding author. Department of Biochemistry and Molecular Biology, University of Oklahoma Health Sciences Center, Oklahoma City, OK, 73126, USA. jialing-lin@ouhsc.edu (J. Lin). **Corresponding author. The State Key Laboratory of Biomembrane and Membrane Biotechnology, Institute of Zoology, Chinese Academy of Sciences, Beijing, 100101, PR China. chenq@ioz.ac.cn (Q. Chen).

[1]These authors contributed equally to this work as co-first authors.

Consent to participate

All authors agree to participate in this MS.

Ethics approval

Not applicable. There are no experiments related to animal or human ethics.

CRediT authorship contribution statement

**Ping Gao:** Formal analysis, designed and carried out most of the experiments, and analyzed most of the data. **Zhi Zhang:** Formal analysis, designed and carried out most of the experiments, and analyzed most of the data. **Rui Wang:** Formal analysis, designed and carried out most of the experiments, and analyzed most of the data. **Li Huang:** Formal analysis, designed and carried out most of the experiments, and analyzed most of the data. **Hao Wu:** participated in immunofluorescence microscopy experiments. **Zhenzhen Qiao:** participated in immunofluorescence microscopy experiments. **Xiaohui Wang:** prepared reagents for most of the experiments. **Haijing Jin:** prepared reagents for most of the experiments, All authors edited the manuscript. **Jun Peng:** developed liposomal membrane permeabilization assay. **Lei Liu:** Supervision, conceived and supervised the project. **Quan Chen:** Supervision, conceived and supervised the project, wrote the manuscript. **Jialing Lin:** Supervision, conceived and supervised the project, wrote the manuscript.

Declaration of competing interest

The authors declare that there is no conflict of interest.

releasing cytochrome *c* from the mitochondria in the cells that lack Bax and Bak, the other proapoptotic perforator. Using liposomal membranes made with typical mitochondrial lipids and reconstituted with purified proteins we revealed this perforation activity was intrinsic to Bcl-2 and could be unleashed by a BH3-only protein, similar to the perforation activity of Bax. Our study thus demonstrated a structural conversion of antiapoptotic Bcl-2 to a proapoptotic perforator through a simple molecular manipulation or interaction that is worthy to explore further for eradicating cancer cells that are resistant to a current Bcl-2-targeting drug.

**Keywords**

Bcl-2 protein pore; Mitochondrial membrane; Cytochrome *c* release; Apoptosis

## 1. Introduction

Bcl-2 family proteins are evolutionarily conserved molecules that play a pivotal role in control of apoptotic protein release from mitochondria.[1–5] They share Bcl-2 homology (BH) domains that are defined by sequence and structural homology and important for their interactions and functions. Antiapoptotic members such as Bcl-2, Bcl-XL and Mcl-1 contain four BH domains (BH1 to 4). Proapoptotic multi-BH members such as Bax, Bak and Bok also contain four BH domains, whereas BH3-only members such as Bid and Bim contain only the BH3 domain. Some BH3-only proteins (termed as activators) directly activate Bax and Bak, inducing their homo-oligomerization and pore formation in the MOM. Other BH3-only proteins (termed as de-repressors or sensitizers) do not bind Bax and Bak. Instead, they bind antiapoptotic proteins to prevent them from binding to and inhibiting the BH3-only activators or the activated Bax and Bak. In contrast, Bok is mainly regulated by ER associated degradation (ERAD) that limits Bok concentration in normal cells. In cells experiencing ER stress that overwhelms the ERAD, Bok concentration increases and accumulates in the mitochondria where it forms pores independent of other Bcl-2 family proteins.[6,7] Surprisingly, structures of multi-BH anti and proapoptotic proteins show remarkable similarity, despite their opposing functions.[8–12] These proteins fold into a helical bundle with a hydrophobic helix (helix 5 in Bcl-2 and Bax) wrapped by multiple amphipathic helices. This structural fold is common among the pore-forming domains of diphtheria toxin and *Escherichia coli* colicins.[13,14] Thus, these proteins and domains may originate from a common ancestor that evolved divergently in sequences, yet, convergently in structures.[15] This structural fold formed by the multi-BH proteins is also formed by Bid,[16,17] a historically named BH3-only protein due to the absence of other BH sequences. Unsurprisingly, Bid was recently shown as the fourth pore-forming protein in the Bcl-2 family, permeabilizing the MOM in cells lacking all the other known proteins of the Bcl-2 family that could potentially activate Bid.[18] Instead, Bid is activated by a proteolysis in the unstructured loop between the first and second helices, an event which was originally found downstream of death receptor activation and carried out by a caspase.[19,20]

Structural similarity implies functional similarity. As an example, Bax and Bcl-2 are structurally similar and both form pores in membranes. During apoptosis initiation soluble Bax is activated by BH3-only activators such as the caspase-cleaved or truncated Bid (cBid

or tBid)[21,22] or the intact Bim.[23] The active Bax integrates into the MOM by embedding helices 5 and 6 partially, and helix 9 fully into the membrane.[24] The integrated Bax forms large oligomeric, perhaps proteolipidic pores that release cytochrome *c* and other larger mitochondrial intermembrane space proteins to the cytosol.[25–33] Bcl-2, which is anchored in the MOM via the C-terminal helix 9 in normal cells, also changes conformation by embedding helix 5 into the membrane after interaction with tBid, Bim or activated Bax.[34–37] While this "activated" Bcl-2 inhibits the large pore formation by Bax, it forms pores in the membrane that are usually smaller than the Bax pore but can be enlarged to accommodate cytochrome *c*.[36–38] We therefore postulated the Embedded Together model to emphasize that the conformational alteration of Bcl-2 family proteins after their interactions at the MOM is a common feature which dictates their pro or antiapoptotic function.[39,40]

One unexpected, yet not surprising, aspect of Bcl-2 family proteins is their interchangeable function in apoptosis regulation. The Bcl-2 homologs in *Drosophila melanogaster* (Debcl/Drob-1) and *Caenorhabditis elegans* (Ced-9) either promote or prevent apoptosis depending on tissue types, apoptotic cues and conformational alterations.[41–45] Mammalian Bcl-2 promotes apoptosis after a caspase cleavage releases the autoinhibition imposed by the N-terminal region.[46] Nur77 interacts with an intrinsically unstructured region of antiapoptotic Bcl-2, converting it to a proapoptotic BH3-only molecule that inhibits Bcl-XL to kill cancer cells via a Bax or Bak dependent mechanism.[47,48] A point mutation in helix 5 of Bcl-XL converts it from a cell protector into a cell killer that may function through a mitochondrial potassium channel.[49] We previously took a chemical biology approach and identified several compounds that can induce cytochrome *c* release and apoptosis in Bax and Bak deficient cells.[37] In particular, a diterpenoid compound elevates the Bim level and its interaction with Bcl-2 converting Bcl-2 to Bax-like oligomers that induce cytochrome *c* release and apoptosis.[37] Also, gossypol interacts with Bcl-2 and triggers conformational changes in Bcl-2 that induce apoptosis independent of Bax and Bak.[50]

Given the structural similarity and the functional plasticity, we hypothesize that alterations of key structural elements that maintain the stereotypical fold of antiapoptotic Bcl-2 could result in a functional conversion of Bcl-2 to a proapoptotic perforator in the mitochondrial membrane. To test this hypothesis we carried out a systematic site-directed mutagenesis of the Bcl-2 fold that is anchored in the MOM by the helix 9 in normal cells but partially embedded into the MOM upon apoptotic induction after a conformational change critical to its antiapoptotic function.[34–36] We identified point mutations that reduce the structural stability of the Bcl-2 fold and convert the antiapoptotic protein to a large pore-forming molecule that releases cytochrome *c* from the mitochondria and induced caspase-dependent apoptosis in Bax and Bak deficient cells. This perforation activity is intrinsic to Bcl-2 as it can be induced by a BH3-only protein in liposomal membranes lacking other cellular proteins. Our study indicates a new anticancer strategy that would kill the Bcl-2 overexpressing cancer cells even if they have eliminated or inactivated both Bax and Bak. Development of a such strategy is increasingly necessary since many leukemia and lymphoma patients who have been treated by Venetoclax, the first Bcl-2-specific inhibitor approved by Food and Drug Administration of United States, National Medical Products Administration of China and equivalent authorities of other countries, have experienced

relapse due to mutations of *bcl-2*, *bax* and/or *bak* genes, or increased expression of *mcl-1* and/or *bcl-xl* genes[51–56] (reviewed in[57,58]).

## 2. Results

### 2.1. Point mutations of Glu$^{152}$ in helix 5 convert antiapoptotic Bcl-2 to a proapoptotic molecule in bax$^{-/-}$/bak$^{-/-}$ cells

To test the hypothesis that mutations in the core region of the stereotypical Bcl-2 fold that dictates its antiapoptotic function could lead to a functional conversion of Bcl-2 to a proapoptotic molecule, we compared the Bcl-2 sequences from four species. The sequence alignment in Fig. 1A shows that the sequences of helix 5 are identical except one conserved change of a valine to an isoleucine in the *Drosophila* sequence. Thus, we carried out alanine-scanning mutagenesis of the extremely conserved helix 5 in the protein core. We tested the apoptotic activity of the resulting Bcl-2 mutants in *HeLa* cells. Following the ectopic expression of the wild-type or mutant Bcl-2, Hoechst staining was used to measure the nuclear condensation, an apoptotic phenotype. Interestingly, the E152A mutant induced apoptosis in more cells compared to the wild-type and the other mutant Bcl-2 (Fig. 1B). We thus investigated the mechanism underlying the ability of the E152 mutant to induce apoptosis.

A key issue is to distinguish whether the Bcl-2 E152 mutant has gained a proapoptotic function or just lost the antiapoptotic function. We reasoned that if it gained a proapoptotic function, the mutant could function as a Bax-like molecule which would induce apoptosis in the absence of Bax and Bak. We thus investigated whether the E152A mutant and other two E152 mutants (E152C and E152S) could induce apoptosis in the absence of Bax and Bak using *Bax*$^{-/-}$/*Bak*$^{-/-}$ mouse embryonic fibroblast (MEF) cells. Since previous studies show that another Bcl-2 helix 5 mutant (G145A) losses the antiapoptotic function,[35,59] we used this mutant, and the wild-type Bcl-2 as controls. Clearly, cell death was observed in all of the E152 mutant-transfected *Bax*$^{-/-}$/*Bak*$^{-/-}$ cells at a similar level as the Bax-transfected cells, while under the same experimental conditions, wild-type Bcl-2 and the G145A mutant had no advert effect on the transfected cells compared to the vector control (Fig. 2A).

We next directly assessed the ability of the Bcl-2 E152 mutants to induce apoptosis in *Bax*$^{-/-}$/*Bak*$^{-/-}$ MEF cells by expression of these proteins with a N-terminal GFP-tag. Hoechst labeling was used to identify pyknotic nuclei, a standard indicator of apoptosis, in the transfected cells identified by GFP fluorescence. The identification of pyknotic nuclei is not affected by differences in the efficiency of transient transfections, because cells were observed at single cell resolution and equal numbers of transfected GFP-positive cells are counted for each group. The cells transfected with the vector that only expresses GFP served as a control to determine the basal rate of death due to the cell culture, transfection, and protein overexpression. As shown in Fig. 2B, the GFP-Bcl-2 E152 mutant-expressing cells displayed condensed and fragmented nuclei, similar to the GFP-Bax-expressing dead cells. These morphological features are distinctly different from the cells expressing the wide-type Bcl-2 or the G145A mutant that maintain intact nuclei, indicative of healthy cells (Fig. 2B). Quantification of apoptotic nuclei revealed that expression of each E152 mutant, like expression of Bax, caused a dramatic increase of apoptotic cells (~15%) compared with

expression of wide-type Bcl-2 or GFP only (~4%) (Fig. 2C). The G145A mutant induced more apoptosis (~7%) than wide-type Bcl-2 but at a significantly lower level than the E152 mutants.

To ascertain that the E152 mutants induced the apoptotic cell death, we measured PARP cleavage by caspases after the cells were transfected with the mutants. The PARP cleavage was detected in the cells expressing the E152 mutants, and to a less extent in those expressing the G145A mutant, but not in those expressing the wild-type Bcl-2 (Fig. 2D). Together with the other apoptotic markers measured above, these measurements clearly demonstrated that the E152 mutants induced typical apoptosis with characteristic morphological and biochemical hallmarks.

To rule out the possibility that the E152 mutant-induced apoptosis was due to nonspecific effect of overexpression of foreign proteins in $Bax^{-/-}/Bak^{-/-}$ cells, we sorted the cells according to the level of GFP whose expression indicated the expression of wild-type or mutant Bcl-2 or Bax. Cells that expressed comparable levels of wild-type or mutant Bcl-2 or Bax as measured by the GFP expression (P3 region in FACS) were collected and assayed for colony formation. Compared to expression of the wild-type Bcl-2 or the G145A mutant or GFP only, expression of the E152 mutants reduced the colony formation of the $Bax^{-/-}/Bak^{-/-}$ cells similar to expression of Bax (Fig. 2E). As expected, the quantitative data from the clonogenic assay (Fig. 2F) inversely correlated with that from the cell morphology-based apoptosis assay (Fig. 2C). These results demonstrated that the Bcl-2 E152 mutants were proapoptotic in the $Bax^{-/-}/Bak^{-/-}$ cells.

### 2.2. Bcl-2 $Glu^{152}$ mutants release cytochrome c from the mitochondria in $bax^{-/-}/bak^{-/-}$ cells

Since the Bcl-2 E152 mutants have gained a proapoptotic function in the $Bax^{-/-}/Bak^{-/-}$ cells, they may act like Bax and Bak to release cytochrome *c* from the mitochondria. We thus immunostained the $Bax^{-/-}/Bak^{-/-}$ MEF cells with a cytochrome c-specific antibody after transfection with the plasmid that expresses GFP-tagged wild-type or mutant Bcl-2. An analysis of confocal fluorescence microscopy images revealed that cytochrome *c* was exclusively localized in the mitochondria in most of the cells expressing GFP-Bcl-2 wild-type, similar to most of the control cells expressing GFP-Bcl-2 G145A or GFP only (Fig. 3A–B). In contrast, most of the cytochrome *c* was released from the mitochondria and diffused into the cytosol in more than half of the cells expressing GFP-Bcl-2 E152 mutants approaching the other control cells expressing GFP-Bax (Fig. 3A–B). The E152 mutants were mainly localized at the mitochondria as wild-type Bcl-2 and the G145A mutant, suggesting that their effects on cytochrome *c* localization and apoptosis are unlikely due to their nonspecific accumulation elsewhere in the cells that may indirectly damage the mitochondria and kill the cells.

### 2.3. The E152 mutations destabilize Bcl-2 structure causing conformational changes to result in Bcl-2 insertion and oligomerization in the mitochondrial membrane

It has been reported that various apoptotic stimuli can elicit conformational changes of Bcl-2 in cells and in membranes.[34–37] Since the Bcl-2 E152 mutants induced apoptosis

and cytochrome *c* release in the absence of Bax and Bak, the mutations might alter the conformation of Bcl-2 resulting in self-association into a cytochrome c-releasing pore in the MOM, as we previously reported for the Bim-activated Bcl-2 [37]. To test this possibility, we used flow cytometry with a specific antibody that recognizes the exposed BH3 motif of Bcl-2 as previously reported[37] to detect this conformational change of Bcl-2 in the $Bax^{-/-}/Bak^{-/-}$ MEF cells. The results showed a drastic increase of the BH3 motif-exposure in the cells expressing the HA-tagged Bcl-2 E152 mutants compared to those expressing the HA-tagged Bcl-2 wild-type or G145A mutant (Fig. 4A).

A previous report has shown that heat alone can activate Bax and Bak to permeabilize the MOM likely by inducing conformational changes of these proapoptotic proteins that lead to their oligomerization and pore formation.[60] We thus measured the thermal stability of recombinant wild-type and mutant Bcl-2 proteins using SYPRO orange dye that fluoresces upon binding to hydrophobic patches in the heat-denatured proteins. Under the same condition in this ThermoFluor assay, different Bcl-2 proteins exhibited different thermal stability (Fig. 4B) as indicated by the melting temperature ($T_m$). The $T_m$ of wild-type Bcl-2 is 56.8 °C while the $T_m$ of the E152S mutant shifts significantly to a lower value of 50.3 °C. The $T_m$ shifts of the E152A and E152C mutants are less but nevertheless to lower values. The downward shift of the melting temperature suggests that the E152 mutations destabilize the Bcl-2 structure. In contrast, the $T_m$ of 56.5 °C for the G145A mutant is very similar to that of the wide-type, suggesting this mutation does not destabilize the Bcl-2 structure. Taken together, these results corroborate that the E152 mutations generate more conformation-altered Bcl-2 proteins in cells by reducing their structural stability.

We next tested whether the Bcl-2 E152 mutants were able to form oligomers in the mitochondria isolated from $Bax^{-/-}/Bak^{-/-}$ cells by incubating the mitochondria with the recombinant wild-type and mutant Bcl-2 proteins whose C-terminal transmembrane sequence was replaced by a hexa-histidine tag (Bcl-2ΔTM-$His_6$), and then treating the samples with a membrane-permeable amine-reactive crosslinker DSS. After immunoprecipitation of the mitochondrial fraction from the E152 mutant samples with an anti-Bcl-2 monoclonal antibody, multiple DSS-crosslinked products were detected by immunoblotting with anti-Bcl-2 polyclonal antibodies. The molecular weights of three Bcl-2 immuno-reactive products are approximately 50, 70 and 100 kDa, corresponding to Bcl-2ΔTM-$His_6$ homodimer, trimer and tetramer or its heterocomplexes with other mitochondrial proteins (Fig. 4C). These Bcl-2ΔTM-$His_6$ complexes were not detected in the wild-type sample, and only one of them was barely detected in the G145A mutant sample. Thus, the capacity of Bcl-2 to form homotypic or heterotypic complexes in the mitochondria is correlated with its cytochrome *c* release activity in the cells (Fig. 3).

We then examined whether the wild-type and mutant Bcl-2ΔTM-$His_6$ proteins that were detected in the mitochondrial fraction were inserted into the mitochondrial membranes. The recombinant wild-type Bcl-2 protein was fully extracted from the mitochondria isolated from $Bax^{-/-}/Bak^{-/-}$ cells by an alkaline buffer that extracts the proteins which fail to insert into the membranes (Fig. 4D). In contrast, most of the E152A and E152S mutants were resistant to the alkaline extraction and thereby inserted into the membranes. However, most of the E152C mutant, like the G145A mutant, was extracted and thereby not inserted. As

expected, the integral mitochondrial membrane proteins COX IV and VADC were fully resistant to the extraction. Since all the recombinant Bcl-2 proteins lack the C-terminal transmembrane domain, the integration of some of them into the membranes would be mediated by other regions. Of note, our previous works have shown that the base of helix 5 of Bcl-2 inserts into the mitochondrial membranes during apoptosis after binding to proapoptotic proteins.[34–37]

Taken the data in this section together, we suggest that the structurally destabilized Bcl-2 E152 mutants are able to change conformation, insert into the mitochondrial membrane and form oligomers to promote cytochrome *c* release in the $Bax^{-/-}/Bak^{-/-}$ cells.

### 2.4. Elimination of a hydrogen bonding network among E152, K22 and S105 that potentially stabilizes the Bcl-2 structural fold unleashes the proapoptotic potential of Bcl-2 in $bax^{-/-}/bak^{-/-}$ cells

Because the E152 mutations reduced the structural stability of Bcl-2, we analyzed a Bcl-2 structure that was previously determined by NMR in solution (PDB entry: 1G5M).[10] As shown in Fig. 5A, the E152 in helix 5 can potentially form two hydrogen bonds; one with the K22 in helix 1 between the hydrogen donor atom NZ of K22 and the hydrogen acceptor atom OE2 of E152, and the other with the S105 in helix 2 between the hydrogen donor atom OG of S105 and the hydrogen acceptor atom OE1 of E152. These hydrogen bonds between the core helix 5 and the peripheral helices 1 and 2 would contribute to the structural stability of Bcl-2 protein. Our thermal stability data from the E152 mutants in comparison with the wild-type support this postulate since the mutations may eliminate these hydrogen bonds, thereby destabilize the protein structure (Fig. 5A).

To provide further support to this postulate and the implication to the protein function, we tested whether the K22A or S105A mutation that would eliminate one of the two hydrogen bonds could also covert Bcl-2 to a proapoptotic molecule in the $Bax^{-/-}/Bak^{-/-}$ MEF cells. Indeed, compared to the cells expressing with GFP-Bcl-2 wild-type protein, more of the cells expressing GFP-Bcl-2 K22A or GFP-Bcl-2 S105A mutant displayed nuclear fragmentation, chromatin condensation, loss of mitochondrial cytochrome *c*, and/or cell shrinkage, similar to the cells expressing GFP-Bcl-2 E152A mutant (Fig. 5B–C). Moreover, similar to the E152A mutant, the K22A and S105A mutants induced PARP cleavage whereas the wild-type Bcl-2 did not (Fig. 5D). These data thus provide further evidence for the importance of a hydrogen bonding network among K22, S105 and E152 in maintaining the Bcl-2 structural fold, destabilization of which can unleash the proapoptotic activity of Bcl-2.

### 2.5. Bcl-2 has an intrinsic large pore-forming activity that can be induced by BH3-only proteins

Our previous study has revealed an intrinsic small pore-forming activity for the recombinant Bcl-2 tethered to liposomal membranes that can be induced by a BH3-only protein tBid to release fluorescent molecules of 0.5 kDa.[36] To determine whether this activity can be enhanced to release larger molecules from liposomes, we improved the purification protocol for the recombinant Bcl-2 protein. We used a high-resolution size exclusion chromatography

that increased the purity of the protein preparation so that we could eliminate the ion exchange chromatography that was used previously in order to achieve the same purity (Fig. 6A–B). This significantly shortened the preparation time and likely enhanced the protein activity. We assayed the pore-forming activity of the resulting Bcl-2 protein using the liposomes that have not only the mitochondrial characteristic phospholipids but also a $Ni^{2+}$--chelating lipid analog in their membranes. Thus, the recombinant Bcl-2 protein that has a $His_6$ tag instead of the hydrophobic helix 9 at the C-terminus can be tethered to the membranes via the $Ni^{2+}$-chelating lipid. The liposomes have fluorescent Cascade Blue dye-conjugated dextran molecules of 10 kDa in their lumen to mimic the cytochrome *c* that has a slightly less hydrodynamic size than the fluorescent dextran molecules.[37] The release of the fluorescent molecules from the liposomal lumen through the pore in the membrane was monitored by antibodies located outside of the liposomes that can bind to the released fluorescent molecules and quench their fluorescence. As shown in Fig. 6C, the fluorescent molecules were gradually released during a time course by the purified recombinant Bcl-2 protein in the presence of the purified tBid protein, and ~40% of the molecules were released by the end of the time course. In comparison, the same concentration of the purified recombinant Bax protein in the presence of the same concentration of the tBid protein released ~65% of the molecules by the end of the time course. In the absence of tBid, neither protein released any molecules during the time course, demonstrating that their large pore-forming activity is induced by this BH3-only protein that binds both proteins to change their conformations and increase their oligomerization.[32,36,38]

Since the E152 mutations in Bcl-2 induced the mitochondrial cytochrome *c* release in the $Bax^{-/-}/Bak^{-/-}$ cells (Fig. 3), we tested if the mutations could induce the large pore formation by the recombinant Bcl-2 protein that can release the fluorescent molecules about the size of cytochrome *c* from the liposomes. Using the purified recombinant E152S mutant protein that was prepared to the same purity as the wild-type protein (Fig. 6A–B), we found that the E152S mutation did not induce the pore formation by Bcl-2 in the absence of tBid (Fig. 6C). In the presence of tBid, the mutant displayed the same pore-forming activity as the wild-type protein. This unexpected result suggests that the liposomes with the truncated Bcl-2 tethered to the membranes via a lipid analog cannot recapitulate what happen to the mitochondria with the full-length Bcl-2 anchored in the membranes by the helix 9. But nevertheless, the liposomal experiments with purified proteins revealed a Bax-like large pore-forming capacity that is intrinsic to Bcl-2 and that can be induced by tBid in the absence of any other cellular proteins.

Since it is well established that Bcl-2 inhibits the large pore formation by Bax,[35,36] we tested whether the recombinant Bcl-2 protein that by itself is capable to form large pores in the liposomal membranes still retains this antiapoptotic activity. Thus, we prepared a liposome sample with both purified Bcl-2 and Bax proteins, each at the same concentration as the samples that were used to assay the pore formation by either protein. As shown in Fig. 6D, the tBid-induced pore-forming activity of both Bcl-2 and Bax is less than the sum of the activities of the individual proteins. This result suggests that the interaction between Bcl-2 and Bax inhibits each other's pore-forming activity. A similar result was obtained when the E152S mutant was combined with Bax, suggesting that the mutation does not affect the Bcl-2 interaction with Bax.

## 3. Discussion

Bcl-2 is well known for its antiapoptotic function, which in part prevents the homo-oligomeric Bax or Bak pore formation by forming heterodimers with these proapoptotic proteins (Fig. 7A). Unlike the homo-oligomers, the heterodimers do not form pores in the MOM. However, the data we presented here reveal a proapoptotic function for Bcl-2. In cells lacking both Bax and Bak, this proapoptotic function of Bcl-2 can be induced by the E152 mutations that destabilize the Bcl-2 structural fold likely by eliminating a hydrogen bonding network. Like Bax and Bak the unstable Bcl-2 mutants change conformation and form homo-oligomeric pores that release cytochrome *c* from the mitochondria, turning the cells to the apoptotic path (Fig. 7B). This proapoptotic function is rooted in an intrinsic pore-forming activity of Bcl-2 that like Bax and Bak shares a structural fold with the α-helical pore-forming bacterial toxins. This intrinsic activity is in display when BH3-only protein tBid interacts the purified recombinant Bcl-2 protein that is tethered the liposomal membrane with a typical mitochondrial lipid composition. Thus, a large, likely oligomeric pore is formed by conformation-changed Bcl-2 proteins, which releases fluorescent molecules of the cytochrome *c* size from the liposome (Fig. 7C). Intriguingly, the E152S mutation that can induce the Bcl-2 pore formation in the mitochondrial membrane within the *bax* and *bak* knockout cell cannot induce the Bcl-2 pore formation in the liposomal membrane, suggesting that the threshold to unleash the pore-forming activity is higher when the Bcl-2 protein lacks the C-terminal transmembrane sequence and the liposomal system lacks other cellular factors.

We can only speculate how Bcl-2 forms pores in the mitochondrial membrane by drawing parallels with Bax and Bak that we have more knowledge about how they form pores. For example, Bax changes conformations after interaction with BH3-only proteins Bim and tBid.[61,62] Like Bax, Bcl-2 also changes conformations after interaction with these BH3-only proteins as we demonstrated previously[35,36] or after destabilizing the Bcl-2 structure as we documented here. Some of the conformational changes are the same among these proteins such as exposure of their BH3 domain (Fig. 4A).[37,61] The conformation-changed Bcl-2 is more embedded in the membranes like the conformation-changed Bax.[24,32,34–36] Also like Bax, Bcl-2 is capable of forming homo-oligomers (Fig. 4C).[28,32,38,63] Since the homo-oligomers of Bax are capable to form pores in the mitochondrial membrane,[32,33] we suggest that the homo-oligomers of Bcl-2 can do the same thing. However, only further experiments can determine whether this suggestion is true, and one of the critical experiments is to determine how Bcl-2 forms the oligomers and how the oligomers engage the mitochondrial membrane.

Bcl-2 is overexpressed in most human cancers, including breast, colon, lung and blood cancers. Elevated Bcl-2 levels correlate with resistance of these cancers to chemotherapeutic drugs.[64–67] Inhibition of Bcl-2 by small molecule compounds has resulted in an anticancer drug, Venetoclax that was approved for leukemia patients.[68,69] Unfortunately, Bcl-2 mutations have emerged in some of the leukemia patients, which reduce the drug binding to Bcl-2, conferring drug resistance and causing relapse.[52,54,70] For example, the affinity for the drug was reduced 180-fold by G101V mutation, whereas the affinity for the BH3 motif of Bim and Bax was only reduced 3 and 8-fold, respectively.[52] Thus, by preferentially

reducing the affinity to drug, this Bcl-2 mutation provided resistance to the therapy. Therefore, new avenues to treat leukemia and other cancers must be explored. We suggest that unleashing the intrinsic pore-forming activity of Bcl-2 by mimicking the effect of E152 mutations on Bcl-2 structural stability or the effect of tBid on Bcl-2 conformation should be high on the list of explorations. Of note, adding E152A mutation to the G101V mutant restored the affinity for Venetoclax, and E152A single mutant had comparable drug binding to the wild-type protein.[70] Thus, the E152A mutation not only retains or restores the drug binding that inhibits the antiapoptotic activity of Bcl-2, it may also unleash the proapoptotic activity of Bcl-2. Therefore, by mimicking this and other E152 mutations one may create a double-edged sword that can eradicate the drug resistant cancer cells more effectively.

## 4. Materials and methods

### 4.1. Cell lines and reagents

*Bax*$^{-/-}$/*Bak*$^{-/-}$ MEF cells were transformed by K-Ras-V12 and E1A. *Bax*$^{-/-}$/*Bak*$^{-/-}$ MEF cells, and *HeLa* cells were cultured in Dulbecco's modified Eagle's medium (DMEM; Gibco BRL, Paisley, United Kingdom) supplemented with 10% heat-inactivated fetal bovine serum (Hyclone, Logan, UT, USA), and 100 U/ml penicillin, 100 μg/ml streptomycin. Cells were maintained in a humidified 5% $CO_2$ atmosphere at 37 °C.

We purchased anti-actin antibody from Sigma (St Louis, MO, USA), anti-Bcl-2, anti-cytochrome c, and anti-PARP antibodies from BD Transduction Labs (Lexington, KY, USA), anti-VDAC1 antibody from Abcam (Cambridge, MA, USA), secondary antibodies from Pharmingen (San Diego, CA, USA), enhanced chemiluminescence (ECL) reagents and cross-linker disuccinimidyl suberate (DSS) from Pierce (Rockford, IL, USA), and all other chemicals from Sigma unless otherwise specified.

### 4.2. Cell fractionation

As described previously,[71] cells were broken with a Dounce homogenizer and the lysate was centrifuged at 1000 *g* for 5 min to remove unbroken cells and nuclei. A further centrifugation at 100,000 *g* for 30 min was used to separate the cytosol from the mitochondria-enriched heavy membranes.

### 4.3. Immunofluorescence microscopy

Cells grown on glass coverslips were stained with 50 nM Mito-Tracker Red CMXRos and 1 μg/mL Hoescht for 15 min at 37 °C. After washed with PBS and fixed in 3.7% formaldehyde-PBS solution, the cells were permeabilized with 0.1% Triton X-100 in PBS for 10 min. After washed with PBS for 3 times, primary antibodies were diluted 100-fold in 1% BSA in PBS and incubated with the permeable cells at 4 °C for overnight. Then, the cells were washed with PBS three times. The FITC-conjugated secondary antibodies were diluted 200-fold in 1% BSA in PBS and incubated with the permeable cells at room temperature for 2 h. The resulting cells were washed with PBS three times. The coverslips were mounted with mounting medium and then imaged by confocal fluorescence microscopy using Zeiss LSM 510 META microscope with excitation/emission wavelengths

of 561/599, 355/460, 488/518 and 488/507 nm to image Mito-Tracker Red, Hoescht, FITC, and GFP, respectively.

### 4.4. Immunoblotting

Cells were washed and lysed in a buffer containing 150 mM NaCl, 25 mM HEPES, pH 7.4, 1% Nonidet P-40, 0.25% sodium deoxycholate, 1 mM EGTA, 1 mM dithiothreitol (DTT), 50 μg/ml trypsin inhibitor, 1 mM phenylmethylsulfonyl (PMSF), 10 μg/mL aprotinin, 10 μg/mL leupeptin, and 10 μg/mL pepstatin. Cell lysates were resolved by using 12% or 15% SDS-PAGE and transferred to nitrocellulose membranes. The membranes were then blocked with PBS containing 5% nonfat dry milk and 0.1% Tween 20 at room temperature for 2 h and probed with indicated antibodies at 4 °C for overnight. The resulting immune complexes were detected with an HRP-conjugated secondary antibody and ECL.

### 4.5. ThermoFluor protein stability assay

The Thermofluor stability assay was performed using the Rotor-Gene 6600 PCR Thermocycler (Corbett Research, Australia). Each sample had a volume of 50 μl with 0.1 mg/ml of purified recombinant wild type or mutant Bcl-2 protein in a buffer (100 mM NaCl, 50 mM $Na_2HPO_4$, 3.8 mM citric acid, pH 7.4). The control sample contained the buffer only. SYPRO orange dye (ThermoFisher Scientific, S6650) was the fluorescent probe and used at 1 × concentration (diluted from the 5000 × stock from the manufacture). The temperature was increased from 25 to 95 °C by 1 °C increment and sustained at each °C for 60 s. The fluorescence signal was recorded using the green channel of the instrument. The midpoint of the protein unfolding transition is defined as the melting temperature ($T_m$).

### 4.6. Preparation of recombinant Bcl-2 proteins

Recombinant human Bcl-2 protein with the C-terminal 22 residues replaced by Leu-Gln-$His_6$ and with or without the E152S mutation was expressed and purified as described[72] with the following modifications. The lysate from a 1-L culture of E. coli cells that express the Bcl-2 protein was incubated with 2 ml of 50% (v/v) of $Ni^{2+}$-NTA agarose at 4 °C for overnight. The resins were packed in a column and washed with ~50 ml of buffer A (50 mM Tris-HCl, pH 8.5, 200 mM NaCl, 1% (v/v) glycerol, 0.2 mM PMSF, 0.15 μg/ml aprotinin, 0.1 μg/ml pepstatin, 0.1 μg/ml leupeptin, 5 mM β-mercaptoethanol) and 20 mM imidazole until $A_{280}$ < 0.05. The Bcl-2 protein was eluted by a series of 2 ml of buffer A with either 40, 60, 80, 100, 200 or 400 mM imidazole, and collected in tubes that already had EDTA so that each of the 2-ml collections will have a final [EDTA] of 10 mM. The collections with $A_{280}$ > 0.1 and Bcl-2 purity >90% as determined by Coomassie Blue staining of SDS-PAGE gels were pooled, and concentrated to $A_{280}$ ~ 6–10 using Centricon centrifugal filter units with a nominal molecular weight limit of 10 kDa. The Bcl-2 protein was further purified by size exclusion chromatography with buffer B (50 mM Tris-HCl, pH 8.5, 200 mM NaCl, 0.5% (v/v) glycerol, 10 mM EDTA) ran through a Superdex 200 Increase 10/300 GL column (GE Healthcare) at a flow rate of 0.8 ml/min. The peak eluted between 16 and 19 ml was collected as 500-μl fractions. The fractions with Bcl-2 purity >95% were combined, concentrated to A280 ~ 3–6, and dialyzed against buffer C (50 mM Tris-HCl, pH 8.5, 140 mM NaCl, 2 mM EDTA, 0.5% (v/v) glycerol) at 4 °C for overnight. After removal of protein aggregates by centrifugation at 10,000 *g* and 4 °C for 5 min, the Bcl-2 protein

concentration was determined from the $A_{280}$ value using a molar extinction coefficient of 43,430 $M^{-1}cm^{-1}$. DTT and glycerol were added to the solution so that the purified Bcl-2 protein was in buffer C with 5 mM DTT and 10% (v/v) glycerol before aliquoting, freezing in liquid nitrogen, and storing at —80 °C.

### 4.7. Liposomal membrane permeabilization by recombinant Bcl-2 proteins

Using an extrusion method as described,[73] liposomes were prepared with chicken egg phosphatidylcholine, chicken trans phosphatidyleth-anolamine, porcine brain phosphatidylserine, soy phosphatidylinositol, and bovine heart cardiolipin (Avanti Polar Lipids) of 46, 28, 9, 9, and 7 mol%, a lipid composition found in Xenopus oocyte mitochondria,[25] plus 1 mol% of 1,2-dioleoyl-*sn*-glycerol-3-{[N(5-amino-1--carboxypentyl)iminodiacetic acid]-succinyl}(nickel salt) (Avanti Polar Lipids), a $Ni^{2+}$-chelating lipid analog that tethers the $His_6$-tagged recombinant Bcl-2 protein to the liposomal membranes. Fluorescent dye Cascade blue (CB)-labeled dextrans of 10 kDa (ThermoFisher Scientific) were encapsulated in the liposomes. The liposomal membrane permeabilization by the recombinant Bcl-2, Bax and/or tBid proteins was monitored by using a method we recently described.[33]

### 4.8. Statistical analysis

Statistical analysis of the data presented in Figs. 2, 3 and 5 was performed using GraphPad Prism 5. Statistical significance of the difference between the means of any two data sets specified in these figures was determined by one-way ANOVA analysis followed by Tukey's multiple-comparisons test. A difference was considered significant when the P value < 0.05. In the figures, a difference between two means with a P value < 0.05, 0.01 or 0.001 is denoted by an *, ** or *** above a line over the corresponding data sets, respectively. A difference between two means with a P value > 0.05 was considered non-significant and denoted by a NS above a line over the corresponding data sets.

Statistical analysis of the data presented in Fig. 6 was performed using GraphPad Prism 9. Statistical significance between the data sets specified in the figure legend was determined by multiple unpaired *t*-test. A difference between the means in the two data sets was considered significant when a P value ≤ 0.05.

## Acknowledgments

This work was supported by National Natural Science Foundation of China Grant (32230046) to Q. C., National Natural Science Foundation of China Grants (92254301) to L. L., US National Institutes of Health Grant (R01GM062964) and Presbyterian Health Foundation Bridge Grant (20221568) to J. L., and by an Institutional Development Award from the National Institute of General Medical Sciences of US National Institutes of Health (P20GM103640).

## References

1. Shamas-Din A, Kale J, Leber B, Andrews DW. Mechanisms of action of Bcl-2 family proteins. Cold Spring Harbor Perspect Biol. 2013;5:a008714. 10.1101/cshperspect.a008714.
2. Hardwick JM, Soane L. Multiple functions of BCL-2 family proteins. Cold Spring Harbor Perspect Biol. 2013;5. 10.1101/cshperspect.a008722.

3. Westphal D, Kluck RM, Dewson G. Building blocks of the apoptotic pore: how Bax and Bak are activated and oligomerize during apoptosis. Cell Death Differ. 2014;21:196–205. 10.1038/cdd.2013.139. [PubMed: 24162660]
4. Czabotar PE, Lessene G, Strasser A, Adams JM. Control of apoptosis by the BCL-2 protein family: implications for physiology and therapy. Nat Rev Mol Cell Biol. 2014;15:49–63. 10.1038/nrm3722. [PubMed: 24355989]
5. Sekar G, Ojoawo A, Moldoveanu T. Protein-protein and protein-lipid interactions of pore-forming BCL-2 family proteins in apoptosis initiation. Biochem Soc Trans. 2022;50:1091–1103. 10.1042/BST20220323. [PubMed: 35521828]
6. Llambi F, et al. BOK is a non-canonical BCL-2 family effector of apoptosis regulated by ER-associated degradation. Cell. 2016;165:421–433. 10.1016/j.cell.2016.02.026. [PubMed: 26949185]
7. Shalaby R, Diwan A, Flores-Romero H, Hertlein V, Garcia-Saez AJ. Visualization of BOK pores independent of BAX and BAK reveals a similar mechanism with differing regulation. Cell Death Differ. 2022:1–11. 10.1038/s41418-022-01078-w.
8. Muchmore SW, et al. X-ray and NMR structure of human Bcl-xL, an inhibitor of programmed cell death. Nature. 1996;381:335–341. 10.1038/381335a0. [PubMed: 8692274]
9. Suzuki M, Youle RJ, Tjandra N. Structure of Bax: coregulation of dimer formation and intracellular localization. Cell. 2000;103:645–654. 10.1016/s0092-8674(00)00167-7. [PubMed: 11106734]
10. Petros AM, et al. Solution structure of the antiapoptotic protein bcl-2. Proc Natl Acad Sci U S A. 2001;98:3012–3017. 10.1073/pnas.041619798. [PubMed: 11248023]
11. Moldoveanu T, et al. The X-ray structure of a BAK homodimer reveals an inhibitory zinc binding site. Mol Cell. 2006;24:677–688. 10.1016/j.molcel.2006.10.014. [PubMed: 17157251]
12. Zheng JH, et al. Intrinsic instability of BOK enables membrane permeabilization in apoptosis. Cell Rep. 2018;23:2083–2094 e2086. 10.1016/j.celrep.2018.04.060. [PubMed: 29768206]
13. Choe S, et al. The crystal structure of diphtheria toxin. Nature. 1992;357:216–222. 10.1038/357216a0. [PubMed: 1589020]
14. Wiener M, Freymann D, Ghosh P, Stroud RM. Crystal structure of colicin Ia. Nature. 1997;385:461–464. 10.1038/385461a0. [PubMed: 9009197]
15. Aouacheria A, Rech de Laval V, Combet C, Hardwick JM. Evolution of Bcl-2 homology motifs: homology versus homoplasy. Trends Cell Biol. 2013;23:103–111. 10.1016/j.tcb.2012.10.010. [PubMed: 23199982]
16. McDonnell JM, Fushman D, Milliman CL, Korsmeyer SJ, Cowburn D. Solution structure of the proapoptotic molecule BID: a structural basis for apoptotic agonists and antagonists. Cell. 1999;96:625–634. 10.1016/s0092-8674(00)80573-5. [PubMed: 10089878]
17. Chou JJ, Li H, Salvesen GS, Yuan J, Wagner G. Solution structure of BID, an intracellular amplifier of apoptotic signaling. Cell. 1999;96:615–624. 10.1016/s0092-8674(00)80572-3. [PubMed: 10089877]
18. Flores-Romero H, et al. BCL-2-family protein tBID can act as a BAX-like effector of apoptosis. EMBO J. 2022;41, e108690. 10.15252/embj.2021108690. [PubMed: 34931711]
19. Luo X, Budihardjo I, Zou H, Slaughter C, Wang X. Bid, a Bcl2 interacting protein, mediates cytochrome c release from mitochondria in response to activation of cell surface death receptors. Cell. 1998;94:481–490. 10.1016/s0092-8674(00)81589-5. [PubMed: 9727491]
20. Li H, Zhu H, Xu CJ, Yuan J. Cleavage of BID by caspase 8 mediates the mitochondrial damage in the Fas pathway of apoptosis. Cell. 1998;94:491–501. 10.1016/s0092-8674(00)81590-1. [PubMed: 9727492]
21. Lovell JF, et al. Membrane binding by tBid initiates an ordered series of events culminating in membrane permeabilization by Bax. Cell. 2008;135:1074–1084. 10.1016/j.cell.2008.ll.010. [PubMed: 19062087]
22. Kim H, et al. Stepwise activation of BAX and BAK by tBID, BIM, and PUMA initiates mitochondrial apoptosis. Mol Cell. 2009;36:487–499. 10.1016/j.molcel.2009.09.030. [PubMed: 19917256]
23. Chi X, et al. The carboxyl-terminal sequence of bim enables bax activation and killing of unprimed cells. Elife. 2020;9. 10.7554/eLife.44525.

24. Annis MG, et al. Bax forms multispanning monomers that oligomerize to permeabilize membranes during apoptosis. EMBO J. 2005;24:2096–2103. 10.1038/sj.emboj.7600675. [PubMed: 15920484]
25. Kuwana T, et al. Bid, Bax, and lipids cooperate to form supramolecular openings in the outer mitochondrial membrane. Cell. 2002;111:331–342. 10.1016/s0092-8674(02)01036-x. [PubMed: 12419244]
26. Schafer B, et al. Mitochondrial outer membrane proteins assist Bid in Bax-mediated lipidic pore formation. Mol Biol Cell. 2009;20:2276–2285. 10.1091/mbc.e08-10-1056. [PubMed: 19244344]
27. Bleicken S, et al. Molecular details of Bax activation, oligomerization, and membrane insertion. J Biol Chem. 2010;285:6636–6647. 10.1074/jbc.Ml09.081539. [PubMed: 20008353]
28. Zhang Z, et al. Bax forms an oligomer via separate, yet interdependent, surfaces. J Biol Chem. 2010;285:17614–17627. 10.1074/jbc.M110.113456. [PubMed: 20382739]
29. Czabotar PE, et al. Bax crystal structures reveal how BH3 domains activate Bax and nucleate its oligomerization to induce apoptosis. Cell. 2013;152:519–531. 10.1016/j.cell.2012.12.031. [PubMed: 23374347]
30. Bleicken S, Landeta O, Landajuela A, Basanez G, Garcia-Saez AJ. Proapoptotic Bax and Bak proteins form stable protein-permeable pores of tunable size. J Biol Chem. 2013;288:33241–33252. 10.1074/jbc.M113.512087. [PubMed: 24100034]
31. Bleicken S, et al. Structural model of active Bax at the membrane. Mol Cell. 2014;56:496–505. 10.1016/j.molcel.2014.09.022. [PubMed: 25458844]
32. Zhang Z, et al. BH3-in-groove dimerization initiates and helix 9 dimerization expands Bax pore assembly in membranes. EMBO J. 2016;35:208–236. 10.15252/embj.201591552. [PubMed: 26702098]
33. Lv F, et al. An amphipathic Bax core dimer forms part of the apoptotic pore wall in the mitochondrial membrane. EMBO J. 2021;40, e106438. 10.15252/embj.2020106438. [PubMed: 34101209]
34. Kim PK, Annis MG, Dlugosz PJ, Leber B, Andrews DW. During apoptosis bcl-2 changes membrane topology at both the endoplasmic reticulum and mitochondria. Mol Cell. 2004;14:523–529. 10.1016/s1097-2765(04)00263-1. [PubMed: 15149601]
35. Dlugosz PJ, et al. Bcl-2 changes conformation to inhibit Bax oligomerization. EMBO J. 2006;25:2287–2296. 10.1038/sj.emboj.7601126. [PubMed: 16642033]
36. Peng J, et al. tBid elicits a conformational alteration in membrane-bound Bcl-2 such that it inhibits Bax pore formation. J Biol Chem. 2006;281:35802–35811. 10.1074/jbc.M608303200. [PubMed: 17005564]
37. Zhao L, et al. Natural diterpenoid compound elevates expression of Bim protein, which interacts with antiapoptotic protein Bcl-2, converting it to proapoptotic Bax-like molecule. J Biol Chem. 2012;287:1054–1065. 10.1074/jbc.Ml11.264481. [PubMed: 22065578]
38. Peng J, et al. Oligomerization of membrane-bound Bcl-2 is involved in its pore formation induced by tBid. Apoptosis. 2009;14:1145–1153. 10.1007/s10495-009-0389-8. [PubMed: 19701793]
39. Leber B, Lin J, Andrews DW. Embedded together: the life and death consequences of interaction of the Bcl-2 family with membranes. Apoptosis. 2007;12:897–911. 10.1007/s10495-007-0746-4. [PubMed: 17453159]
40. Leber B, Lin J, Andrews DW. Still embedded together binding to membranes regulates Bcl-2 protein interactions. Oncogene. 2010;29:5221–5230. 10.1038/onc.2010.283. [PubMed: 20639903]
41. Xue D, Horvitz HR. Caenorhabditis elegans CED-9 protein is a bifunctional cell-death inhibitor. Nature. 1997;390:305–308. 10.1038/36889. [PubMed: 9384385]
42. Colussi PA, et al. Debcl, a proapoptotic Bcl-2 homologue, is a component of the Drosophila melanogaster cell death machinery. J Cell Biol. 2000;148:703–714.10.1083/jcb.148.4.703. [PubMed: 10684252]
43. Igaki T, et al. Drob-1, a Drosophila member of the Bcl-2/CED-9 family that promotes cell death. Proc Natl Acad Sci U S A. 2000;97:662–667. 10.1073/pnas.97.2.662. [PubMed: 10639136]
44. Hengartner MO, Horvitz HR. Activation of C. elegans cell death protein CED-9 by an amino-acid substitution in a domain conserved in Bcl-2. Nature. 1994;369:318–320. 10.1038/369318a0. [PubMed: 7910376]

45. Senoo-Matsuda N, Igaki T, Miura M. Bax-like protein Drob-1 protects neurons from expanded polyglutamine-induced toxicity in Drosophila. EMBO J. 2005;24:2700–2713. 10.1038/sj.emboj.7600721. [PubMed: 16001086]
46. Cheng EH, et al. Conversion of Bcl-2 to a Bax-like death effector by caspases. Science. 1997;278:1966–1968. 10.1126/science.278.5345.1966. [PubMed: 9395403]
47. Lin B, et al. Conversion of Bcl-2 from protector to killer by interaction with nuclear orphan receptor Nur77/TR3. Cell. 2004;116:527–540. 10.1016/s00928674(04)00162-x. [PubMed: 14980220]
48. Kolluri SK, et al. A short Nur77-derived peptide converts Bcl-2 from a protector to a killer. Cancer Cell. 2008;14:285–298. 10.1016/j.ccr.2008.09.002. [PubMed: 18835031]
49. Szabo I, Soddemann M, Leanza L, Zoratti M, Gulbins E. Single-point mutations of a lysine residue change function of Bax and Bcl-xL expressed in Bax- and Bak-less mouse embryonic fibroblasts: novel insights into the molecular mechanisms of Bax-induced apoptosis. Cell Death Differ. 2011;18:427–438. 10.1038/cdd.2010.112. [PubMed: 20885444]
50. Lei X, et al. Gossypol induces Bax/Bak-independent activation of apoptosis and cytochrome c release via a conformational change in Bcl-2. Faseb J. 2006;20:2147–2149. 10.1096/fj.05-5665fje. [PubMed: 16935937]
51. Fresquet V, Rieger M, Carolis C, Garcia-Barchino MJ, Martinez-Climent JA. Acquired mutations in BCL2 family proteins conferring resistance to the BH3 mimetic ABT-199 in lymphoma. Blood. 2014;123:4111–4119. 10.1182/blood-2014-03-560284. [PubMed: 24786774]
52. Blombery P, et al. Acquisition of the recurrent Gly101Val mutation in BCL2 confers resistance to venetoclax in patients with progressive chronic lymphocytic leukemia. Cancer Discov. 2019;9:342–353. 10.1158/2159-8290.CD-18-1119. [PubMed: 30514704]
53. Blombery P, et al. Characterization of a novel venetoclax resistance mutation (BCL2 Phe104Ile) observed in follicular lymphoma. Br J Haematol. 2019;186:e188–e191. 10.1111/bjh.16069. [PubMed: 31234236]
54. Blombery P, et al. Multiple BCL2 mutations cooccurring with Gly101Val emerge in chronic lymphocytic leukemia progression on venetoclax. Blood. 2020;135:773–777. 10.1182/blood.2019004205. [PubMed: 31951646]
55. Blombery P, et al. Clonal hematopoiesis, myeloid disorders and BAX-mutated myelopoiesis in patients receiving venetoclax for CLL. Blood. 2022;139:1198–1207. 10.1182/blood.2021012775. [PubMed: 34469514]
56. Moujalled DM, et al. Acquired mutations in BAX confer resistance to BH3-mimetic therapy in Acute Myeloid Leukemia. Blood. 2022. 10.1182/blood.2022016090.
57. Xu Y, Ye H. Progress in understanding the mechanisms of resistance to BCL-2 inhibitors. Exp Hematol Oncol. 2022;11:31. 10.1186/s40164-022-00283-0. [PubMed: 35598030]
58. Lew TE, Seymour JF. Clinical experiences with venetoclax and other pro-apoptotic agents in lymphoid malignancies: lessons from monotherapy and chemotherapy combination. J Hematol Oncol. 2022;15:75. 10.1186/s13045-022-01295-3. [PubMed: 35659041]
59. Yin XM, Oltvai ZN, Korsmeyer SJ. BH1 and BH2 domains of Bcl-2 are required for inhibition of apoptosis and heterodimerization with Bax. Nature. 1994;369:321–323. 10.1038/369321a0. [PubMed: 8183370]
60. Pagliari LJ, et al. The multidomain proapoptotic molecules Bax and Bak are directly activated by heat. Proc Natl Acad Sci U S A. 2005;102:17975–17980. 10.1073/pnas.0506712102. [PubMed: 16330765]
61. Gavathiotis E, Reyna DE, Davis ML, Bird GH, Walensky LD. BH3-triggered structural reorganization drives the activation of proapoptotic BAX. Mol Cell. 2010;40:481–492. 10.1016/j.molcel.2010.10.019. [PubMed: 21070973]
62. Dengler MA, et al. BAX activation: mutations near its proposed non-canonical BH3 binding site reveal allosteric changes controlling mitochondrial association. Cell Rep. 2019;27:359–373 e356. 10.1016/j.celrep.2019.03.040. [PubMed: 30970242]
63. Zhang Z, et al. Bcl-2 homodimerization involves two distinct binding surfaces, a topographic arrangement that provides an effective mechanism for Bcl-2 to capture activated Bax. J Biol Chem. 2004;279:43920–43928. 10.1074/jbc.M406412200. [PubMed: 15302859]

64. Hanahan D, Weinberg RA. Hallmarks of cancer: the next generation. Cell. 2011;144:646–674. 10.1016/j.cell.2011.02.013. [PubMed: 21376230]

65. Cory S, Huang DC, Adams JM. The Bcl-2 family: roles in cell survival and oncogenesis. Oncogene. 2003;22:8590–8607. 10.1038/sj.onc.l207102. [PubMed: 14634621]

66. Letai AG. Diagnosing and exploiting cancer's addiction to blocks in apoptosis. Nat Rev Cancer. 2008;8:121–132. 10.1038/nrc2297. [PubMed: 18202696]

67. Yip KW, Reed JC. Bcl-2 family proteins and cancer. Oncogene. 2008;27:6398–6406. 10.1038/onc.2008.307. [PubMed: 18955968]

68. Merino D, et al. BH3-Mimetic drugs: blazing the trail for new cancer medicines. Cancer Cell. 2018;34:879–891. 10.1016/j.ccell.2018.ll.004. [PubMed: 30537511]

69. Souers AJ, et al. ABT-199, a potent and selective BCL-2 inhibitor, achieves antitumor activity while sparing platelets. Nat Med. 2013;19:202–208. 10.1038/nm.3048. [PubMed: 23291630]

70. Birkinshaw RW, et al. Structures of BCL-2 in complex with venetoclax reveal the molecular basis of resistance mutations. Nat Commun. 2019;10:2385. 10.1038/s41467-019-10363-1. [PubMed: 31160589]

71. Zheng Y, et al. Essential role of the voltage-dependent anion channel (VDAC) in mitochondrial permeability transition pore opening and cytochrome c release induced by arsenic trioxide. Oncogene. 2004;23:1239–1247. 10.1038/sj.onc.1207205. [PubMed: 14647451]

72. Kim KM, et al. Biophysical characterization of recombinant human Bcl-2 and its interactions with an inhibitory ligand, antimycin A. Biochemistry. 2001;40:4911–4922. 10.1021/bi002368e. [PubMed: 11305906]

73. Tan C, et al. Auto-activation of the apoptosis protein Bax increases mitochondrial membrane permeability and is inhibited by Bcl-2. J Biol Chem. 2006;281:14764–14775. 10.1074/jbc.M602374200. [PubMed: 16571718]

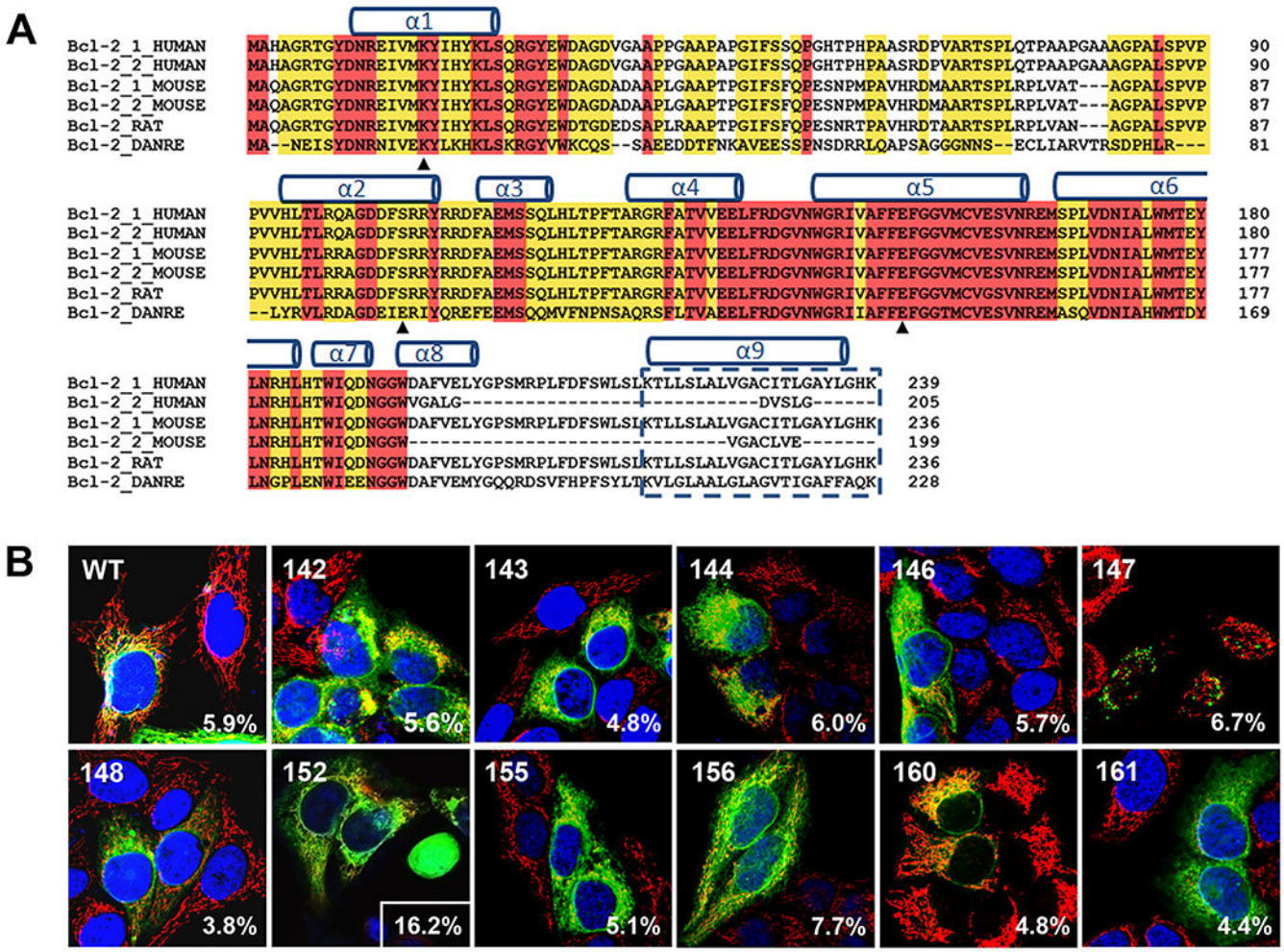


**Fig. 1. Alanine scanning mutagenesis suggests that E152 in α5-helix of Bcl-2 plays a role in apoptosis regulation by Bcl-2 in *HeLa* cells.**

(A) Amino acid sequence alignment of Bcl-2 from human (two isoforms), mouse (two isoforms), rat, and Drosophila (denoted by Bcl-2_DROME). The residues that are identical and highly conserved are highlighted in red and yellow, respectively. The α-helical regions (α1, α2, etc.) are indicated above the alignment with cylinders. The C-terminal transmembrane regions are enclosed in a dashed box. The three amino acid residues that form a potential hydrogen bonding network in the Bcl-2 structure (illustrated in Fig. 5A) are indicated below the alignment with triangles. (B) Apoptosis of *HeLa* cells expressing Bcl-2. Alanine mutagenesis was carried out with human Bcl-2 gene inserted in pSG5 vector. The resulting plasmids were used to transiently transfected *HeLa* cells for 48 h to express HA-tagged Bcl-2 wide-type (WT) or the mutants that are indicated by the sequence number of the residue that was changed to an alanine. The cells were then stained with anti-HA antibody and FITC-conjugated secondary antibody, Hoechst 33342, and MitoTracker, and subjected to confocal microscopy analysis. Representative confocal images from three independent experiments are shown with green, blue and red colors assigned to the three fluorescent dyes, respectively. The numbers of apoptotic cells were determined by propidium iodide and Annexin V-FITC staining using flow cytometry, and the

average percentages of the apoptotic cells from three independent experiments are shown in the lower right corner of the images. Scale bar corresponds to 20 μm.

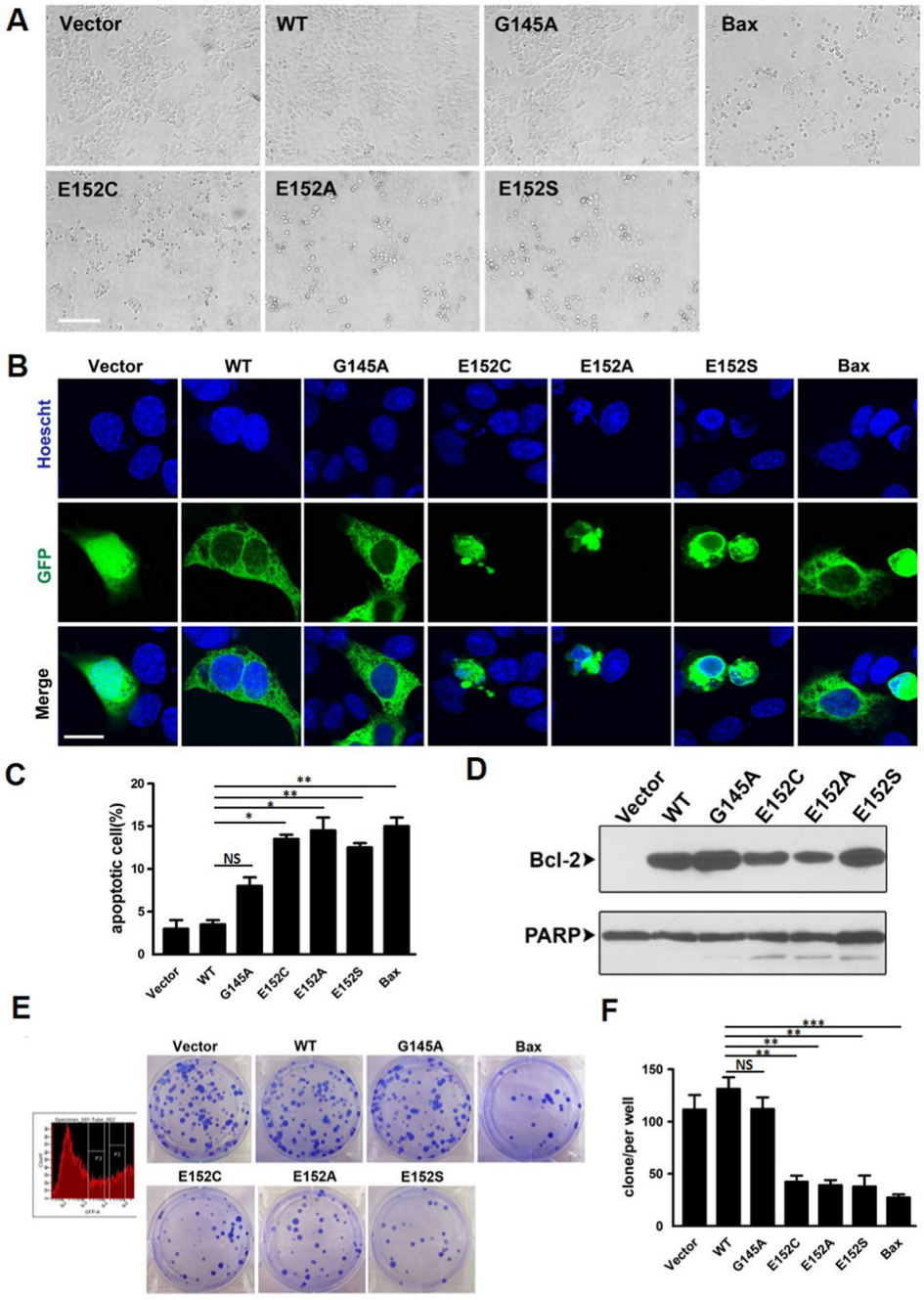


**Fig. 2. Bcl-2 E152 mutants induced apoptosis in *Bax*$^{-/-}$/*Bak*$^{-/-}$ cells.**

(A) The plasmid that expresses GFP-tagged wide-type (WT) or the indicated mutant Bcl-2, or Bax, or the control vector that expresses GFP only was used to transfect *Bax*$^{-/-}$/*Bak*$^{-/-}$ MEF cells. After 48 h, the morphology of the cells was examined by light field microscopy. Representative images from one of three independent experiments are shown. Scale bar corresponds to 200 μm. (B) The *Bax*$^{-/-}$/*Bak*$^{-/-}$ MEF cells were transfected with the plasmid that expresses GFP-tagged wide-type or the indicated mutant Bcl-2, or Bax, or the control vector that expresses GFP only. After 48 h, the cells were stained with Hoechst 33342,

and fluorescence images were collected by confocal microscopy. Representative images from one of three independent experiments are shown. Scale bar represents 20 μm. (C) Three-hundred cells from each of the indicated groups that displayed GFP fluorescence in an independent experiment described in (B) were examined for nuclear condensation. The percentage of the cells that were apoptotic was calculated and shown as mean ± SD for that group from three independent experiments. (D) The $Bax^{-/-}/Bak^{-/-}$ MEF cells were transfected with the plasmid that expresses HA-tagged wide-type or the indicated mutant Bcl-2, or the control vector. After 48 h, full-length PARP and caspase-cleaved PARP were detected by immunoblotting with an anti-PARP antibody. The total intensity of the PARP band(s) indicates the protein loading from each sample. The levels of different HA-Bcl-2 proteins in these samples were determined by immunoblotting with the anti-HA antibody. The data shown were from one of three independent experiments. Similar data were obtained from the other experiments. (E) The $Bax^{-/-}/Bak^{-/-}$ MEF cells were transfected the plasmid that expresses GFP-tagged wide-type or the indicated mutant Bcl-2, or Bax, or the control vector that expresses GFP only. After 48 h, the cells were sorted by FACS and the histogram is shown on the left side. The cells through P3 gate were collected and seeded on six-well plates. Colonies of cells formed after 5-day culture were visualized by crystal violet staining. Representative images from three independent experiments are shown on the right side. (F) The numbers of cell colonies from the experiments described in (E) were scored. The means ± SD from three independent experiments are shown. Statistical significance of a difference between the means of the data sets that are indicated by a line above them was determined using one-way ANOVA followed by Tukey's multiple-comparisons test, and *, ** or *** above the line indicates the resulting P value < 0.05, 0.01 or 0.001, respectively. NS above the line indicates a non-significant difference between the means of the indicated data sets with a P value > 0.05.

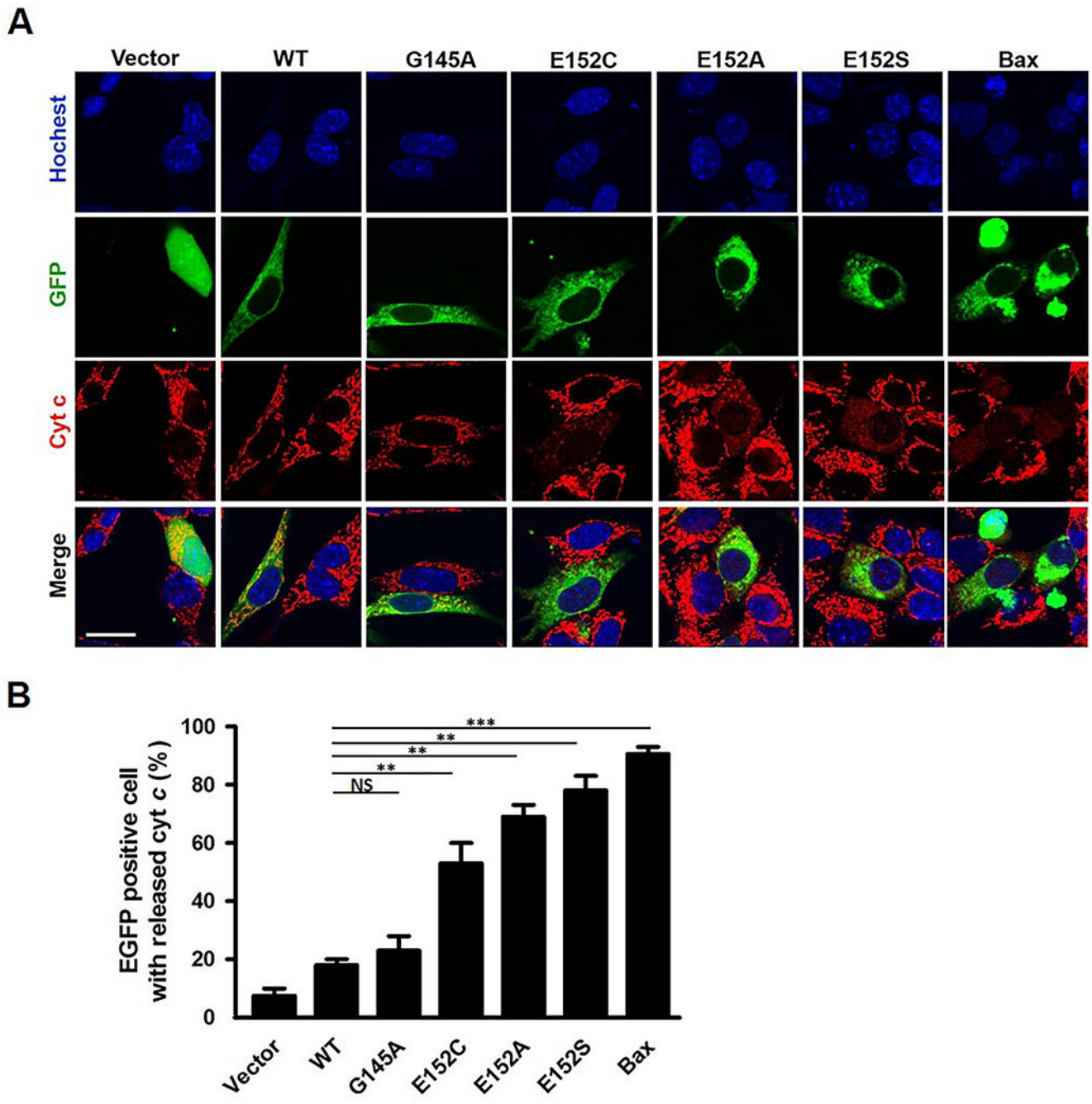


**Fig. 3. Bcl-2 E152 mutants released cytochrome *c* from the mitochondria in *Bax*$^{-/-}$/*Bak*$^{-/-}$ cells.**

(A) The *Bax*$^{-/-}$/*Bak*$^{-/-}$ MEF cells were transfected with the plasmid that expresses GFP-tagged wide-type or the indicated mutant Bcl-2, or Bax, or the control vector that expresses GFP only. After 48 h, the cells were stained with an anti-cytochrome c antibody, PE-conjugated secondary antibody and Hoechst 33342. Fluorescence images were collected by confocal microscopy. Representative images from one of three independent experiments are shown. Scale bar represents 20 μm. (B) Two-hundred cells from each of the indicated groups that displayed GFP fluorescence in an independent experiment described in (A)

were examined for the cytochrome *c* that were released from the mitochondria and diffused throughout the cells. The percentage of the cells that released cytochrome *c* was calculated and shown as mean ± SD for that group from three independent experiments. Statistical significance of a difference between the means of the data sets that are indicated by a line above them was determined using one-way ANOVA followed by Tukey's multiple-comparisons test, and ** above the line indicates the resulting P value < 0.01. NS above the line indicates a non-significant difference between the means of the indicated data sets with a P value > 0.05.

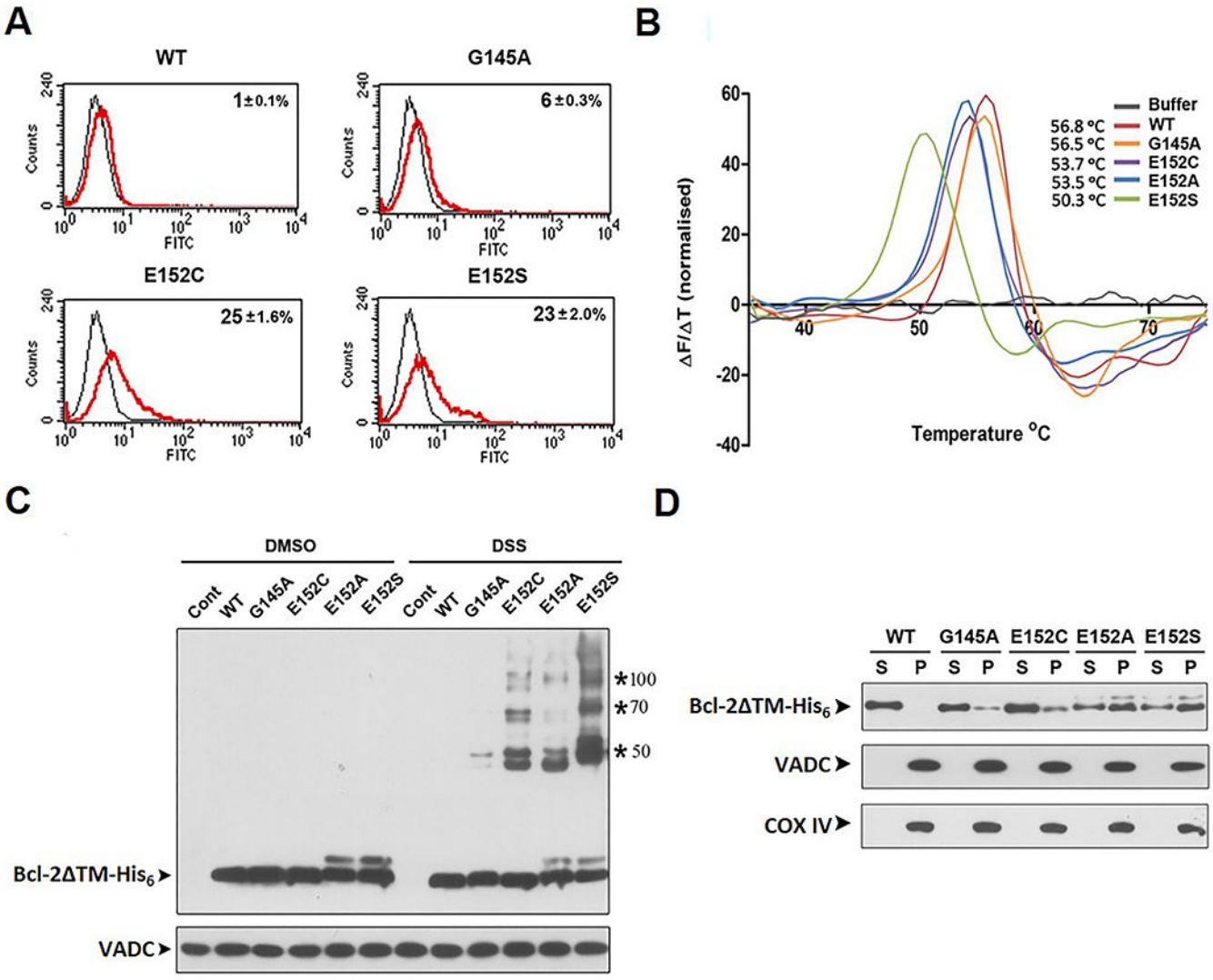


**Fig. 4. Structure-destabilized and conformation-changed Bcl-2 E152 mutants form membrane-inserted oligomers in *Bax*$^{-/-}$/*Bak*$^{-/-}$ mitochondria.**

(A) The *Bax*$^{-/-}$/*Bak*$^{-/-}$ MEF cells were transfected with the plasmid that expresses HA-tagged wide-type or the indicated mutant Bcl-2, or the control vector that expresses HA only. After 48 h, the cells were immunostained with a Bcl-2 BH3 domain specific antibody and a FITC-conjugated secondary antibody, and analyzed by flow cytometry. The cell counts versus the FITC fluorescence intensity histograms obtained from the cells that were side-by-side transfected with the vector or the indicated Bcl-2 plasmid in one of the three independent experiments are shown in black or red, respectively. The mean percentage ± SD of each Bcl-2 plasmid-transfected cells that displayed Bcl-2 immunofluorescence over the background fluorescence from three independent experiments is indicated in the respective histogram. (B) Thermal stability of purified recombinant wild-type and mutant Bcl-2 proteins. The curves are the first derivatives of the fluorescence variations of SYPRO orange dye against temperature at different temperatures, and color-coded for the indicated Bcl-2 proteins and the buffer control. The temperature corresponding to the peak of each curve is the melting temperature of each Bcl-2 protein, and listed beside its color code.

(C) One-hundred nM of purified recombinant wide-type or mutant Bcl-2 proteins were incubated with the mitochondria isolated from the *Bax*$^{-/-}$/*Bak*$^{-/-}$ MEF cells at 30 °C for 30 min. For the control, no Bcl-2 protein was incubated with the mitochondria. After centrifugation, the mitochondrial fraction from each incubation was split to two with one treated with the crosslinker DSS and the other with the vehicle DMSO for 30 min. All the samples were immunoprecipitated with an anti-Bcl-2 monoclonal antibody and analyzed by immunoblotting with anti-Bcl-2 polyclonal antibodies. The asterisks on right side of the blot indicate the three crosslinking products with the approximate molecular weights in kDa indicated. The immunoblot for VDAC in each sample serves as the loading control. (D) The indicated purified recombinant Bcl-2 proteins were incubated with the isolated mitochondria at 30 °C for 30 min. The mitochondria were then pelleted and treated with 0.1 M $Na_2CO_3$ (pH 11.5) for 20 min. The samples were centrifuged to separate the alkaline extracted (S) and non-extracted (P) fractions. Bcl-2 proteins in these fractions were detected by the immunoblotting and the results are shown in the top panel. The PVDF membrane used in the Bcl-2 immunoblotting was then stripped and re-immunoblotting for VDAC and Cox IV, and the results are shown in the bottom panels, serving as the mitochondrial integral membrane protein and the loading controls.

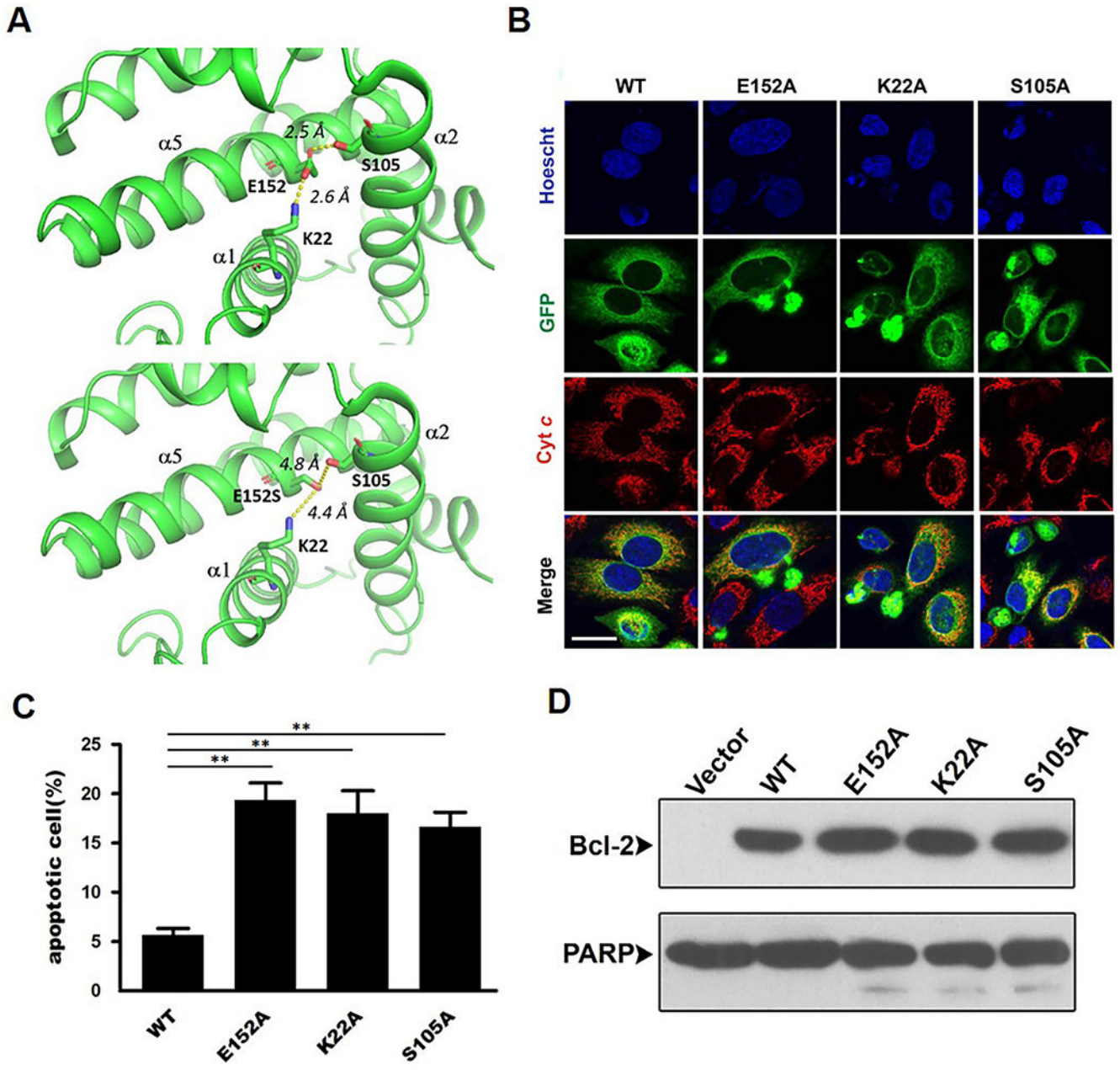


**Fig. 5. Disruption of a hydrogen bonding network formed by the E152, K22 and S105 in the Bcl-2 structure unleashes its proapoptotic activity.**

(A) Potential hydrogen bonds between the sidechain atoms of K22, S105, and E152 in a Bcl-2 structure (PDB entry: 1G5M). In the wild-type structure created in PyMOL, the three residues in stick form are projected from the α-helices 1, 2 and 5 (α1, α2, and α5) in ribbon form. The hydrogen bonding atoms are link by dashed lines with the distance between them indicated in Å. The mutant structures were generated in PyMOL using the Mutagenesis wizard for protein. While the alanine mutation of each of the three residues eliminates the hydrogen donor or acceptor atom, the serine mutation of E152 keeps a potential hydrogen acceptor OG; however, the distance between the S152 OG and the

potential hydrogen donor of the K22 NZ or S105 OG is too long to form a hydrogen bond. (B) The *Bax*$^{-/-}$/*Bak*$^{-/-}$ MEF cells were transfected with the plasmid that expresses either GFP-Bcl-2 wide-type or the indicated mutant. After 48 h, the cells were stained with an anti-cytochrome c primary antibody, PE conjugated secondary antibody and Hoechst 33342, and their fluorescent images were collected by confocal microscopy. Representative images from one of three independent experiments are shown. Scale bar represents 20 μm. (C) Three-hundred cells from each of the indicated groups that displayed GFP fluorescence in an independent experiment described in (B) were examined for nuclear condensation. The percentage of the cells that were apoptotic was calculated and shown as mean ± SD for that group from three independent experiments. (D) The *Bax*$^{-/-}$/*Bak*$^{-/-}$ MEF cells were transiently transfected with HA-Bcl-2 wide-type, K22A, S105A, E152 mutants, and control vector. After 48h, full-length PARP and caspase-cleaved PARP were detected by immunoblotting with the specific antibody. The levels of PARP served as the protein loading control for the experiment. The expression levels of Bcl-2 and its mutants were detected by immunoblotting with a Bcl-2 specific antibody. Results shown are representative of three independent experiments with very similar results. Statistical significance of a difference between the means of the data sets that are indicated by a line above them was determined using one-way ANOVA followed by Tukey's multiple-comparisons test, and ** above the line indicates the resulting P value < 0.01.

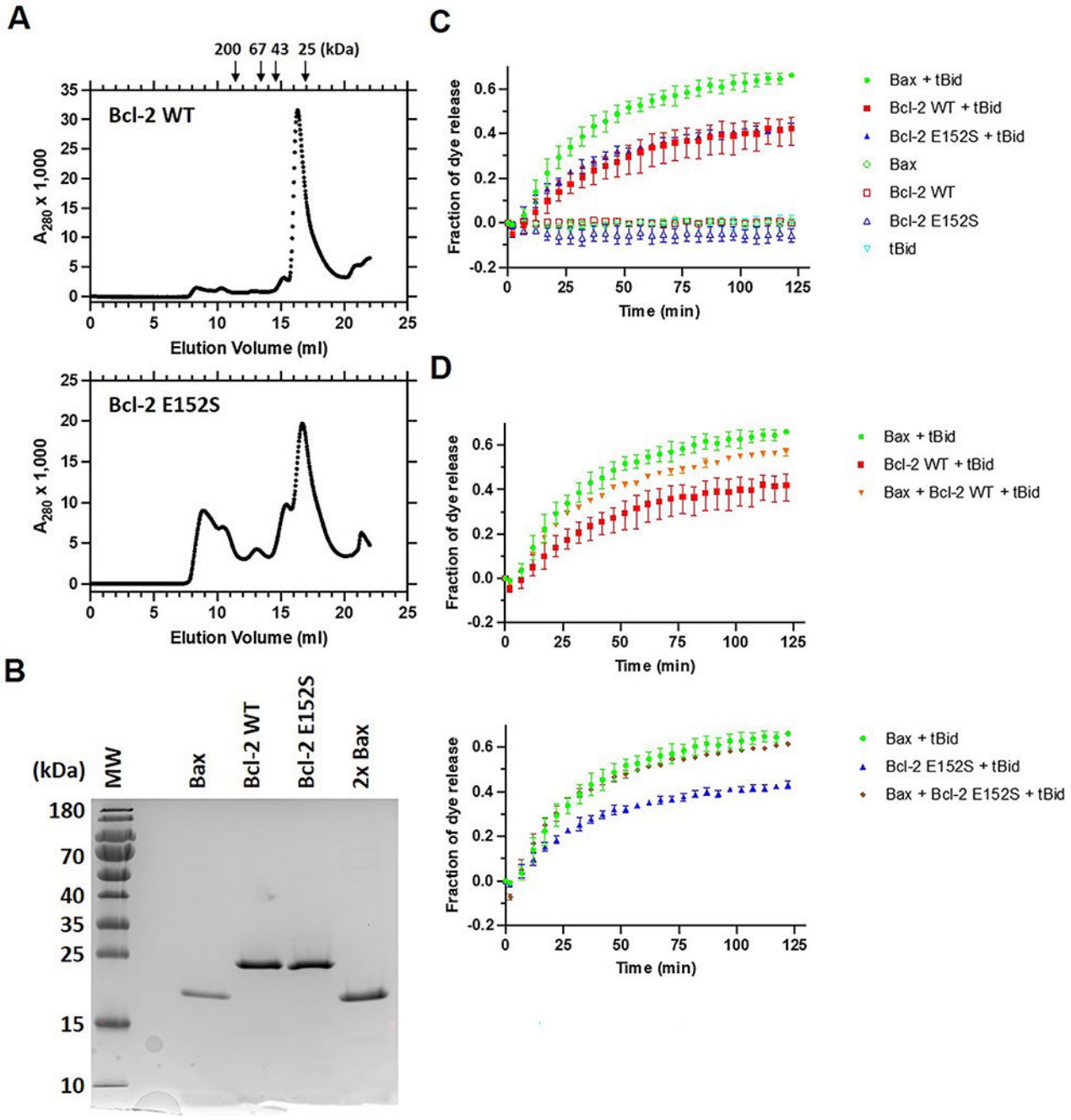


**Fig. 6. Large pore formation by purified recombinant Bcl-2 proteins in liposomal membranes can be induced by a BH3-only protein.**

(A) Size-exclusion chromatograms of recombinant Bcl-2 proteins. The indicated recombinant Bcl-2 proteins with the C-terminal hydrophobic helix 9 replaced by a $His_6$ tag were purified by their affinity to Ni-NTA agarose resins, and then further purified by size-exclusion chromatography. The eluted proteins were detected by their absorbance at 280 nm ($A_{280}$). Since the peak fractions eluted between 16 and 19 ml were expected to contain monomeric Bcl-2 proteins based on the elution volumes of the protein markers whose molecular weights in kDa are indicated on the top of the chromatograms, the

proteins in these fractions were analyzed by SDS-PAGE and Coomassie Blue staining. The fractions with 95% or more Bcl-2 proteins were pooled. (B) 135 pmole of the indicated recombinant Bcl-2 proteins pooled from the peak fractions described in (A) were analyzed by SDS-PAGE and Coomassie Blue staining alongside with the purified Bax protein of 135 or 270 pmole (indicated by 2x Bax), and the PageRuler prestained protein ladder (ThermoFisher Scientific) with the molecular weights (MW) in kDa indicated. (C–D) The release of the fluorescent dye-conjugated dextran molecules from the liposomes containing 12.5 μM of mitochondrial lipids and 0.125 μM of $Ni^{2+}$-chelating lipid analog by 50 nM of $His_6$-tagged Bcl-2 wild-type (WT) or E152S mutant protein, or 50 nM of Bax protein in the absence or presence of 15 nM of tBid protein was monitored during a 122-min time course by dye-specific antibodies that quenches the fluorescence of the released molecules. The fraction of the dye release was determined by the fluorescence reduction caused by the protein(s) and normalized to that caused by 0.1% of Triton X-100 that solubilized all the liposomes and released all the fluorescent molecules. The data shown are means and ranges from three replicates with the “Bcl-2 WT + Bid” sample and two replicates with other samples. The data from the “Bcl-2 WT or E152S + tBid” and “Bax + tBid” samples shown in (C) are also shown in (D) to compared with the data from the “Bcl-2 WT or E152S + Bax + tBid” samples. Multiple unpaired t tests were performed with the following data sets to determine whether the difference between the means is significant as indicated by the P values ≤ 0.05. The fractions of the dye release are significantly different between Bcl-2 WT, Bcl-2 E152S or Bax + and − tBid samples after 22, 12 or 22 min, respectively, demonstrating that the pore-forming activity of each is induced by tBid. The fractions of the dye release are not significantly different between Bcl-2 WT and Bcl-2 E152S samples through the entire time course, no matter whether tBid is present, demonstrating that the mutation does not induce or enhance Bcl-2 pore formation in the liposomal membrane.

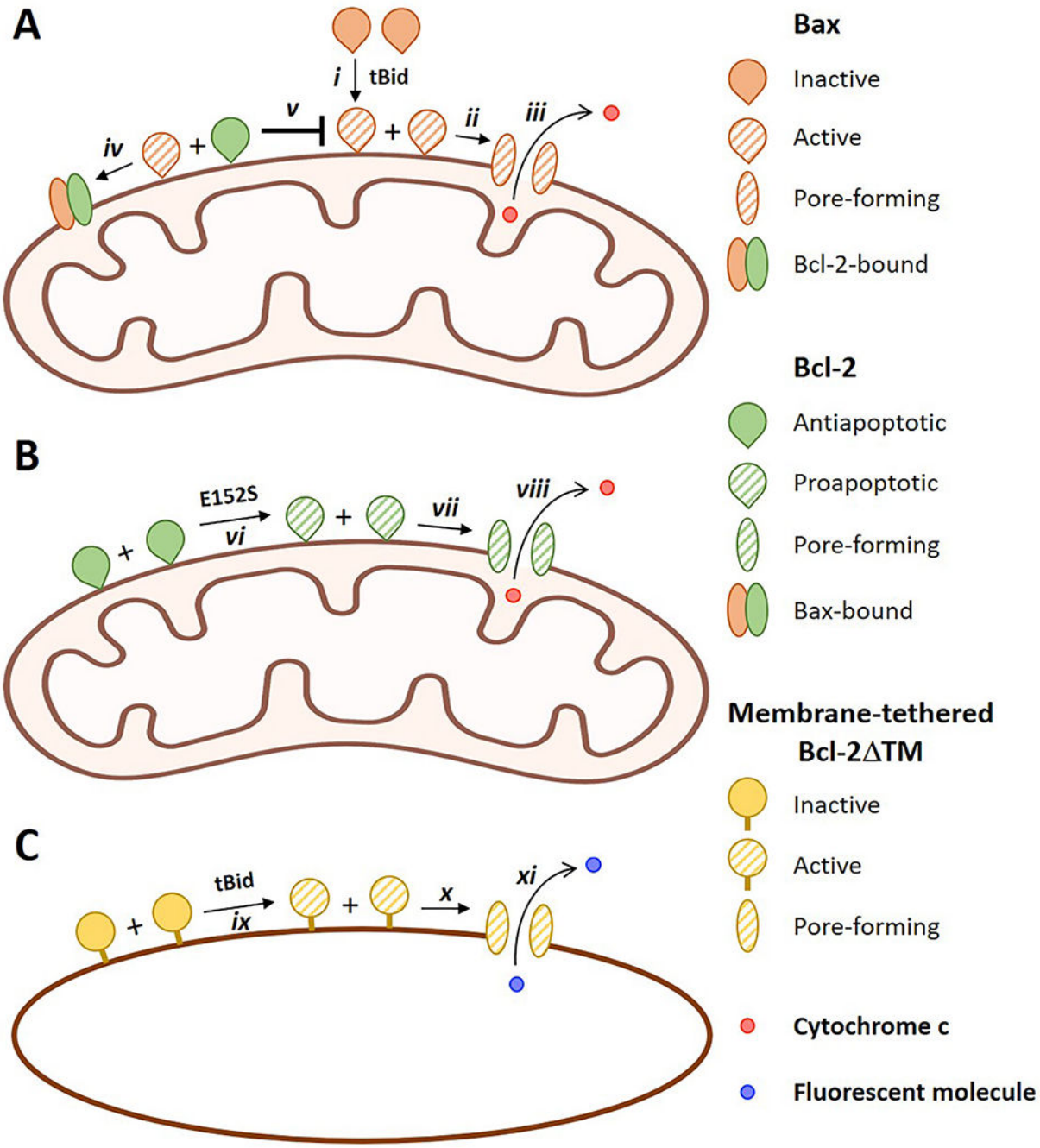


**Fig. 7. A model for functional conversion of antiapoptotic Bcl-2 to a Bax-like proapoptotic pore-forming molecule.**

(A) In cells that have Bax, Bcl-2 functions as an antiapoptotic protein. In these cells, a BH3-only protein such as tBid interacts with Bax changing it from an inactive soluble conformation to an active conformation that inserts into the mitochondrial outer membrane (*step i*) The active Bax proteins associate with one another, and form an oligomeric pore (*step ii*) that releases cytochrome c to the cytoplasm (*step ii*), initiating apoptotic cell death. The antiapoptotic Bcl-2 binds the active Bax (*step iv*) to prevent it from forming the oligomeric pore with the other Bax (*step v*), thereby inhibiting the cytochrome *c* release and

apoptosis. (B) In cells lacking Bax (and Bak), a mutation such as E152S can destabilize the antiapoptotic Bcl-2 structure converting it to a proapoptotic molecule (*step vi*). The proapoptotic Bcl-2 acts like the active Bax forming an oligomeric pore in the mitochondrial membrane (*step vii*) that releases cytochrome *c* (*step viii*) and initiates apoptosis. (C) For a recombinant Bcl-2 protein that lacks the C-terminal transmembrane sequence but is tethered to the liposomal membrane of a typical mitochondrial lipid composition, its pore-forming potential can be unleashed by tBid. Thus, tBid activates the Bcl-2 proteins by inducing conformational changes (*step ix*) so that they can assemble an oligomeric pore (*step x*) that releases fluorescent molecules of the size of cytochrome *c* from the liposome (*step xi*). BioRender was used to create the schematics of mitochondria.